

An Investigation into Mechanism of XiangDan Injection for the Improvement of Inflammation and Oxidative Stress in Patients with Acute Myocardial Ischemia

Zizheng Wu¹, Xing Chen¹, Jiahao Ye¹, Xiaoyi Wang¹, Zhixi Hu^{1,*}

¹College of Chinese Medicine, Hunan University of Chinese Medicine, No. 300, Bachelor Road, Yuelu District, Changsha, Hunan, 410208, China

*Corresponding author: 003405@hnucm.edu.cn

Keywords: XiangDan injection; Acute myocardial ischemia (AMI); Network pharmacology; Molecular docking; Inflammatory response; UPLC-Q-TOF-MS

Abstract: This study aimed to investigate the protective effects and mechanism of Xiangdan injection (XDI) in treating acute myocardial ischemia (AMI) induced by isoproterenol (ISO). To this end, this study employed UPLC-Q-TOF-MS technology, network pharmacology, molecular docking technology, and animal experiment verification. Based on the review of the research literature, XDI absorption into blood components was screened and verified using the UPLC-Q-TOF-MS technology. The software Cytoscape 3.7.2 and the Applied Protein-Protein Interaction Network Analysis Database (STRING) were utilized to build a protein-protein interaction (PPI) network. The software examines the gene ontology (GO) and Kyoto Encyclopedia of Genes and Genomes (KEGG) pathway to identify common targets. Autodock vina software was used to verify the molecular docking between the main active ingredients and key targets. A rat model of AMI was developed through the intraperitoneal injection of XDI at low and high doses (2.7 and 5.4 ml/kg) for 7 consecutive days, 85 mg/kg of isoproterenol was injected subcutaneously into the back of the rats On the 6th day. The UPLC-Q-TOF-MS analysis revealed that XDI absorbed 9 blood components. The results also showed that 128 common targets were found in the "XDI-AMI" combination. KEGG enrichment analysis demonstrated that the treatment of AMI by XDI may be related to disease pathways such as lipid and atherosclerosis and TNF signaling pathway. The study findings suggested that XDI can improve the function of cardiomyocytes and, thereby, treat AMI by regulating oxidative stress and inflammatory responses.

1. Introduction

AMI is the pathophysiological basis of angina, coronary heart disease, and myocardial infarction[1]. During the ischemic phase of the heart, cellular oxidative metabolism is suppressed, cellular homeostasis is disrupted, and the body experiences intricate biological responses such as

oxidative stress, inflammation, and fibrosis.

XDI is a solution composed of fragrant rosewood (*Dalbergia odorifera* T. C. Chen) and danshen (*Salvia bowleyana*) that dilates blood vessels and increases coronary blood flow[2]. *Dalbergia odorifera* T. C. Chen is the dried heartwood of the trunk and root of *Dalbergia odorifera* T. C. Chen; it possesses various beneficial properties such as antioxidant, cardiovascular, antithrombotic platelet aggregation, antitumor, anti-inflammatory, antibacterial, and central nervous system inhibition effects[3]. Recent studies have found that danshen has cardiovascular, antitumor, antioxidant, antifibrotic, antidiabetic, and other effects, and its main components are water-soluble salvianolic acids and fat-soluble tanshinone[4].

The mechanism of action of XDI (fragrant rosewood, *Dalbergia odorifera* T. C. Chen and danshen, *Salvia bowleyana*) in the treatment of AMI has not yet been clarified. Therefore, this study employs UPLC-Q-TOF-MS, network pharmacology, molecular docking, and other experiments to verify the mechanism of action of XDI in improving inflammation and oxidative stress caused by AMI.

2. Material

2.1 Animals

Fifty SPF male SD rats (6-8 weeks old, 180-220 g) were provided from Hunan Slack Jingda Laboratory Animal Co., Ltd. (certificate No. SCXK2019-0004) and kept in the Animal Experiment Center of Hunan University of Traditional Chinese Medicine. The subjects were acclimated to feeding in an environment with a temperature of 22±2°C and relative humidity ranging from 50% to 70% under a 12-hour day-night cycle; they had unrestricted access to food. The experiment was approved by the Animal Ethics Committee of Hunan University of Traditional Chinese Medicine (HUCMS21-2403-53).

2.2 Reagents

Rat Superoxide Dismutase (SOD) Assay Kit (Cat. No.: AF3262-A), Rat Reactive Oxygen Species (ROS) Kit (Cat. No. AF3686-A), Rat Lactate Dehydrogenase (LDH) Kit (Cat. No. AF3480-A), Rat Malondialdehyde (MDA) Kit (Cat. No. AF8503-A), interleukin 6 (IL-6) antibody kit (stock number: AF3066-A; Rat Cardiac Troponin I (cTn-I) Kit (Cat. No. AF3686-A), Rat IL-10 Kit (Cat. No. AF3071-A), Hematoxylin-eosin staining (HE) staining kit, Masson's staining solution kit, Methanol (TEDIA, lot: 23125027), and acetonitrile (TEDIA, lot: 23125140) were used as reagents.

2.3 Instruments

The instruments used in the study were as follows: UPLC-Q-TOF-MS (Waters, USA, model: Xevo G2-XS Qtof), Masslynx V4.2 Chromatography Mass Spectrometry Workstation (Waters, USA), dehydration machine (DIAPATH, model number: Donatello), burburied machine (Wuhan Junjie Electronics Co., Ltd., model: JB-P5), pathology slicome (Shanghai Leica Instruments Co., model: RM2016), frozen platform (Wuhan Junjie Electronics Co., Ltd., model: JB-L5)

3. Methods

3.1 Preparation of drugs and medicated serum

3.1.1 Drugs

XDI (Shenwei Pharmaceutical Group Co., Ltd., Guoyao Zhunzi Z13020793, batch number: 230814C1); propranolol (Pro) (production batch: E231235), and isoproterenaline (production batch: F2215417, stock number: I129810) were used in this study.

3.1.2 Medicated serum

SPF SD rats were initially housed and then relocated for 7 days. Following the provided guidelines, the maximum clinical dosage of XDI was determined to be 20 ml per day. Additionally, the appropriate conversion equation for body surface area between experimental animals and humans was established. Consequently, the XDI group received an intraperitoneal injection dosage of 1.8 ml/kg/d, administered once a day for 7 days. SD rats in the blank serum group were gavaged with an equal volume of normal saline once a day for 7 days. Following the last period of fasting, blood was collected from the abdominal aorta. After the serum was separated, 500 μ L of the serum sample was taken for further processing. To this end, 1500 μ L of pre-cooled methanol-acetonitrile (1:1) was added to the serum sample. The mixture was then vortexed for 3 minutes and centrifuged at 13,000 rpm for 10 minutes at 4°C. In the next step, 1500 μ L of the supernatant was concentrated by nitrogen blowing until dry. Then 1500 μ L of 70% methanol was added to the mixture and then it was vortexed for 3 min and centrifuged for 15 min (13,000 rpm, 4°C). Finally, the supernatant was placed in a liquid phase vial for LC-MS analysis.

3.2 UPLC-Q-TOF-MS analysis

3.2.1 Preparation of test solution

For this purpose, 1.0 mL of XDI was placed in a 5.0-mL measuring flask, the volume was fixed with ultrapure water, and filtered through a 0.22- μ m microporous membrane. The LC-MS analysis was then performed in liquid-phase vials.

3.2.2 XDI blood component analysis

The chromatographic conditions were as stated: The ACQUITY UPLC@BEH C18 Column had a particle size of 1.7 μ m and dimensions of 2.1 mm \times 50 mm (50 mm \times 2.1 mm, 1.8 μ m). It was operated at a temperature of 40°C. The mobile phase used in this experiment consisted of a mixture of water containing 0.05% formic acid (A) and methanol (B). The elution process involved a gradient, with the proportion of methanol increasing over time. Specifically, the gradient was as follows: from 0 to 6 minutes, the proportion of methanol increased from 7% to 15%; from 6 to 11 minutes, it increased from 15% to 25%; from 11 to 20 minutes, it increased from 25% to 50%; from 20 to 25 minutes, it increased from 50% to 80%; from 25 to 28 minutes, it was 100% methanol; and from 28 to 30 minutes, it decreased back to 5% methanol. The temperature of the column was 30°C. The volume flow rate was 0.2 milliliters per minute; the post-column shunt ratio was 3 to 1; and the injection volume was 20 μ L and 1 μ L, respectively.

The conditions for mass spectrometry were as follows: The electrospray ion source (ESI) was used to scan a range of m/z 100~1500 in both positive and negative ion detection modes. The capillary voltage was set to 3.0kV for positive ions and 2.5kV for negative ions. The nozzle voltage was set to 40V, and the dry gas velocity was set to 800L/h. The ion source temperature was maintained at 120°C. Argon was used as the collision gas, and the collision energy was ranged between 20 and 50eV.

3.3 Network pharmacological analysis

3.3.1 XDI active ingredient target collection

The PubChem database was used to search for the smiles number associated with the active ingredient in the blood. The Swiss Target Prediction database was then employed to predict the target of interest.

3.3.2 Prediction of targets related to AMI

The keyword "acute myocardial infarction" was searched on the DisGeNET database (<https://www.disgenet.org>) and GeneCards database (<http://www.genecards.org>). The GeneCards screening criteria required a relevance score of at least 10, while the DisGeNET screening criteria required a score of at least 0.1. After merging the results, duplicate gene targets were removed to obtain the final set of gene targets for acute myocardial infarction (AMI).

3.3.3 Development of a protein-protein interaction (protein-protein interaction, PPI) network

The targets obtained by "XDI-AMI" were inserted into the STRING database (<https://www.string-db.org/>), the "multiple proteins" function was selected, and the protein species was determined to be "Homo sapiens". A PPI network of XDI therapeutic AMI targets was developed to facilitate visual analysis of core targets. The analysis results were saved in a tsv file and imported into Cytoscape 3.7.2 software.

3.3.4 Development of a network diagram of "drug-active ingredient-common target".

The XDI active ingredients, targets, pathways, and diseases obtained above were inserted into Cytoscape 3.7.2 for visualization processing. This involved developing the "XDI-active ingredient-common target" network model for treating AMI using XDI treatment. The aforementioned models were then analyzed using parameters such as degree and betweenness.

3.3.5 Gene Ontology (GO) functional enrichment analysis and Kyoto Encyclopedia of Genes and Genomes (KEGG) pathway enrichment analysis

The targets of XDI were inserted into the Bioconductor database and RX64 4.0.4 software, and the core target genes were analyzed by GO functional enrichment analysis and KEGG pathway enrichment analysis. The GO enrichment analysis focused on biological processes (BP), cell composition (CC), and molecular function (MF). Bar charts and bubble charts were developed to visualize the results.

3.3.6 Molecular docking validation

The main core compounds in the "XDI-active ingredient-common target" network were selected for molecular docking with the target. The SDF file for the primary target protein was obtained from the PubChem database (<https://pubchem.ncbi.nlm.nih.gov/>). The SDF file was then converted to mol2 format using OpenBabel software. Subsequently, the proteins were subjected to dehydration, hydrogenation, and charge calculation using AutoDockTools 1.5.6. The resulting data was saved as a pdbqt file, serving as a pair acceptor. The structure of the core protein was obtained through the PDB database (<http://www.rcsb.org/>), and the ligands and water molecules were removed in Pymol. The protein structure and compound molecules were then docked in Autodock Vina, and finally, the results were visualized and analyzed in Discover Studio 4.5.

3.4 Experimental verification

3.4.1 Grouping, modeling, and administration

After 7 days of acclimatization, 50 rats were randomly divided into 5 groups (n=10): ctrl group, model group, propranolol group, XDI-L group, and XDI-H group. The dosage was determined according to the equivalent equation of the body surface area between experimental animals and humans, and the intraperitoneal injection doses of XDI-L and XDI-H were 2.7ml/kg and 5.4ml/kg, respectively, which were 1.5 and 3 times of the highest clinical dose. The propranolol group received a dose of 10 mg/kg/d administered orally, while the ctrl group and model group were given an equivalent volume of normal saline for 7 consecutive days. The subjects in the XDI-L, XDI-H, Pro, and model groups were administered a subcutaneous injection of ISO (85 mg/kg) in the back two hours after the administration on the sixth day. The ctrl group received a subcutaneous injection of the same volume of normal saline for two consecutive days. Twenty-four hours after the modeling was completed, the subjects were anesthetized to take blood samples from their abdominal aorta. Their heart was also removed and rinsed with normal saline and placed on ice; the left ventricle was frozen at -80°C, and the rest of the heart tissue was fixed with 4% paraformaldehyde to be subsequently used for measuring the relevant indicators.

3.4.2 Measurement of the serum level of LDH, cTn-I, ROS, IL-10, IL-6, and TNF- α

The blood samples were left at room temperature for 2 hours and then they were centrifuged at 3500 rpm for 15 min at 4°C. After extracting the supernatant, the serum levels of LDH, cTn-I, ROS, IL-10, IL-6, and TNF- α were measured by ELISA.

3.4.3 Determination of MDA and SOD activity in myocardial tissue

A sample of myocardial tissue was ground with normal saline at a ratio of 1:9. The mixture was then centrifuged at 2,500 rpm for 10 minutes. The supernatant was collected as the tissue homogenate. Then the MDA and SOD activity in the homogenate was measured using a biochemical method.

3.4.4 HE staining for observing myocardial pathological changes

The heart tissue was preserved using a 4% paraformaldehyde solution. The tissue was dehydrated using a series of alcohol solutions with concentrations of 75%, 80%, 95%, and 100%. It was then

made transparent using xylene, soaked in paraffin, and embedded into tissue blocks. The tissue blocks were cut into 7- μ m sections using a microtome. The sections were deparaffinized and rehydrated using xylene. HE staining was performed, followed by mounting with neutral gum. Finally, the tissue sections were observed and photographed under a microscope.

3.4.5 Masson's staining

The solution of hematoxylin-iron complex is applied to the tissue for 5 minutes, followed by rinsing with running water. Then, we need to add Ponceau S solution and let it sit before rinsing with water. Next, apply phosphomolybdic acid stain to differentiate the stain, removing excess stain by tapping off the solution. Afterward, we need to stain with Toluidine blue for 2 minutes, rinse with running water, and then wash the slides with 1% glacial acetic acid. We need to place the slides in glacial acetic acid for 1 minute, dehydrate in 100% ethanol for 1 minute, and air dry.

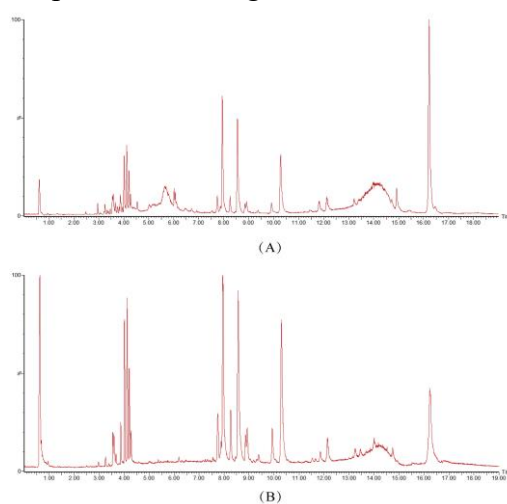
3.4.6 Statistical analysis

The data were statistically analyzed in SPSS-24.0. One-way analysis of variance (ANOVA) and then the Turkey-Kramer test were performed to compare the groups. The experimental data were expressed as mean \pm standard deviation ($\bar{x} \pm s$). A statistically significant difference was shown by a $P < 0.05$.

4. Results

4.1 UPLC-Q-TOF-MS mass spectral acquisition

Biological samples were qualitatively analyzed using UPLC-Q-TOF-MS. The total ion current plot (TIC) of the samples in both positive and negative ion modes is shown in Figure 1.



Note: (A: the positive mode of contained medicine serum; B: the negative mode of contained medicine serum)

Figure 1: Total ion chromatograms

4.2 XDI blood components and serum medicinal chemical analysis

The blood samples contained 451 active ingredients in medicated serum, 9 active ingredients in medicated serum, 290 active ingredients in XDI injection, and 240 active ingredients in the blank serum group. The results are presented in a Venn diagram (see Figure2).

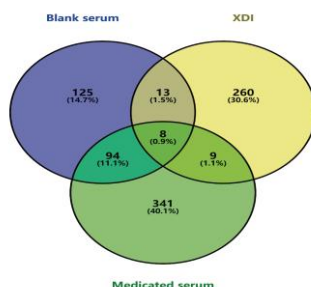


Figure 2: Venn diagram of effective blood component of XDI

4.3 Analysis of absorbed blood components

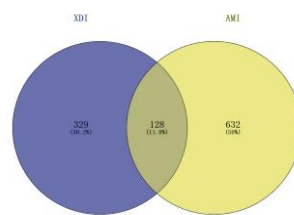
After testing and analysis, 9 kinds of XDI components were obtained (see Table 1).

Table 1: Components identified in XDI by UPLC-Q-TOF-MS.

NN _o	tR/min	Identification	Formula	Selected ion	Expected	Detected	M/Z	Error (ppm)	Fragment ion MS ²
11	4.55	Monomethyl lithospermate	C ₂₈ H ₂₄ O ₁₂	[M-H]-	552.1268	552.1257084	551.1184319	1.9376	309.0784
22	0.60	6-O-galloylarbutin	C ₁₉ H ₂₀ O ₁₁	[M+K]+	424.1006	424.0985	463.0617	-4.42	259.0827; 313.0588
33	10.41	Butylphthalide	C ₁₂ H ₁₄ O ₂	[M+e]+	190.0994	190.0999	190.0993	2.65	103.0608; 130.0742
44	4.28	Periplocoside D	C ₇₀ H ₁₁₂ O ₂₆	[M+OH]+	1368.7442	1368.7443	1351.7411	0.12	147.0578; 191.0875; 800.4337
55	6.06	Periplocoside E	C ₆₅ H ₁₀₆ O ₂₄	[M+e]+	1270.7074	1270.7017	1270.7011	-4.52	144.0876; 525.3268; 613.3866; 995.5334
66	4.42	Periplocoside K	C ₆₈ H ₁₀₈ O ₂₆	[M+NH ₄] +	1340.7129	1340.7061	1358.7400	-4.97	613.3861; 995.5334
77	2.96	Esculentoside I	C ₄₉ H ₇₈ O ₂₂	[M-Cl]-	1018.4985	1018.4997	1053.4691	1.18	281.0721; 222.0497; 112.9850
88	2.49	Lithospermic acid	C ₂₇ H ₂₂ O ₁₂	[M-H]-	538.1111	538.1089	537.1017	-4.08	493.1125; 293.0426
99	8.93	Tunicyclin A	C ₂₉ H ₄₅ N ₇ O ₁₁	[M-H]-	667.3177	667.3147	666.3074	-4.53	552.3098; 463.2218

4.4 Construction of XDI targets, AMI-related targets, and "XDI-AMI" common targets

After testing and analysis, a total of 9 XDI components were obtained. After eliminating duplicate targets, a total of 457 targets were obtained. From the Genecards database, 745 AMI targets were screened. Additionally, 32 targets were screened out from the DisGeNET database. The disease database was merged, and duplicate targets were subsequently removed. In the end, a total of 760 disease target genes were obtained. A total of 124 "XDI-AMI" common targets were screened by PERL software and visualized by VENNY plots, as shown in Figure 3.

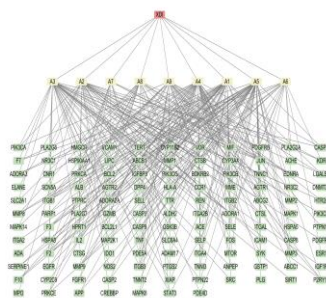


Note: The blue color represents the targets of XDI, the yellow color represents the targets of AMI, and the middle part represents their common targets.

Figure 3: Venn diagram visualizing the common targets of "XDI-AMI"

4.5 XDI "Drug-Active Ingredient-Common Target" Network Analysis

The core active ingredients were screened according to the degree value, and the results showed that the core targets of XDI in the treatment of AMI were as follows: lithospermate ,lithospermic acid, Esculentoside I, 6-O-galloylarbutin, Butylphthalide, and Tunicyclin A (see Figure 4).

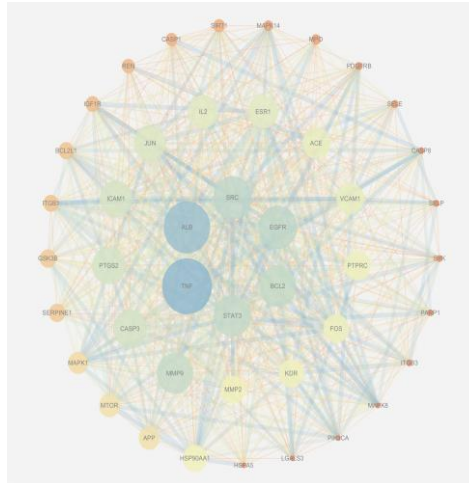


Note: Red represents XDI, yellow represents the active ingredients, and green represents the common targets of "Chinese medicine disease"

Figure 4: Network of "XDI-active component-common target"

4.6 PPI Network Analysis

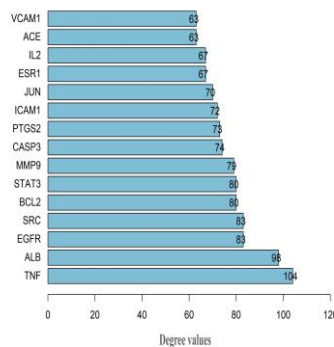
The PPI analysis revealed the involvement of 128 nodes and 2,167 edges. The mean node degree was 33.9, while the mean local clustering coefficient was 0.594 (see Figure 5).



Note: The higher the Degree value, the bluer the circle color and the larger the area. The lower the degree value, the more reddish the circle color and the smaller the area. The higher the combined score value, the thicker the connection between the two points and the bluer the connection color. The lower the combined score value, the thinner the line between the two points and the redder the line color.

Figure 5: PPI network diagram of the common targets of XDI and AMI(Degree \geq 50)

RX64 4.0.4 was used to depict the histograms of the first 30 target genes and visualize the histograms. The core targets were screened according to the degree value, and the results showed that the core targets of XDI in the treatment of AMI were TNF, ALB, EGFR, BCL2, SRC, and STAT3 (see Figure 6).



Note: The abscissa represents the degree value, and the ordinate represents the gene name

Figure 6: Core target map of the top 15 degree values

4.7 GO enrichment and KEGG pathway enrichment analysis

The GO enrichment analysis yielded 2,217 biological process (BP) entries, primarily associated with diverse biological processes including leukocyte migration, positive regulation of response to external stimulus, and response to lipopolysaccharide(see Figure 7). A total of 110 cell component (CC) entries were obtained, which were mainly related to various cell components such as membrane raft, membrane microdomain, and external side of plasma membrane. Moreover, there were a total of 156 molecular function (MF) items, which were mainly related to various molecular functions such as endopeptidase activity, serine hydrolase activity, and protease binding (see Figure 8)

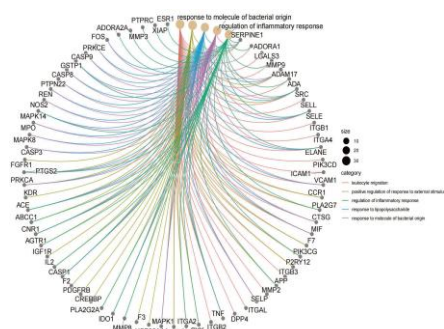


Figure 7: Relationship between BP and targets.

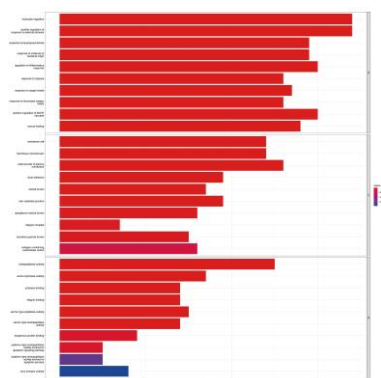


Figure 8: GO analysis results.

The results demonstrated the presence of 171 KEGG biological pathways that were mainly enriched in XDI pathways for the treatment of AMI. They were related to lipid and atherosclerosis, AGE-RAGE signaling pathway in diabetic complications, TNF signaling pathway, and other disease pathways (see Figure 9).

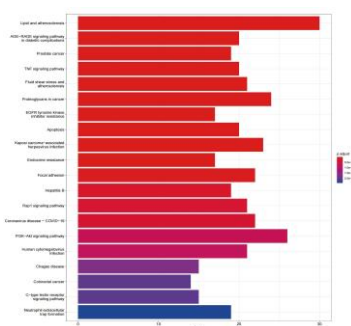
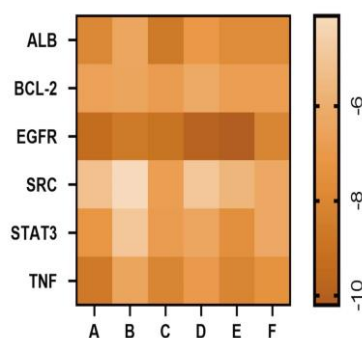


Figure 9: Results of KEGG pathway enrichment analysis.

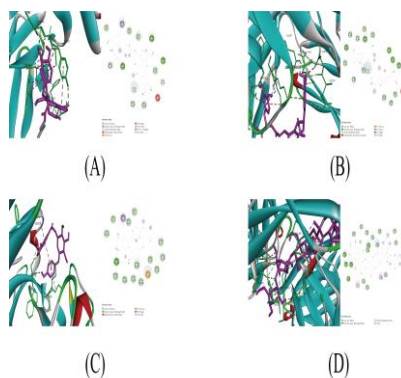
4.8 Molecular docking results

The results showed that the optimal docking score was obtained for EGFR- Monomethyl lithospermate (-10.2 kcal/mol), EGFR-Lithospermic acid (-9.9 kcal/mol), followed by EGFR-6_O_galloylarbutin (-9.3 kcal/mol) and EGFR-Esculentoside I (-9 kcal/mol). The results indicated that the above-mentioned active ingredient-target docking showed good binding force. Figure 10 shows the results of docking active ingredients into the blood and target protein molecule, and Figure 11 presents the molecular docking diagram.



Note: A: 6_O_galloylarbutin; B: Butylphthalide; C: Esculentoside I; D:Lithospermic acid; E: Monomethyl lithospermate; F: Tunicyclin A

Figure 10: Heatmap of the docking core targets of XDI molecules



(A)EGFR-Monomethyl lithospermate; (B)EGFR-Lithospermic acid;(C)EGFR-6_O_galloylarbutin; (D)EGFR-Esculentoside I

Figure 11: Results of molecular docking diagram

4.9 HE staining results

As shown in Figure 12, the cardiomyocytes were normal, the myocardial fibers were slightly arranged neatly, the myocardial fibers were uniformly stained, and the myocardial cell space was normal in the control group. In addition, myocardial cells were severely hypertrophied, myofiber arrangement was severely disordered, myocardial cell space was severely widened, and myocardial tissue was severely atherosclerosis with significant collagenization in the model group. The cardiomyocytes were slightly hypertrophied and the muscle fibers were slightly disordered in the Pro group. The results also demonstrated that myocardial cells were moderately hypertrophied, myocardial fibers were moderately disordered, myocardial fibers were thickened, and myocyte space was moderately widened in the XDI-L group. Moreover, mild hypertrophy of cardiomyocytes, mild disordered arrangement of myocardial fibers, and a slight widening of myocardial cell space were observed in the XDI-H group.

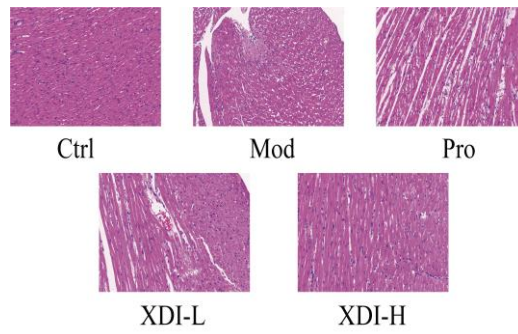


Figure 12: HE staining

4.10 Masson's staining results

Figure 13 and Table 2 demonstrate the utilization of Masson's staining to identify collagen fibers in muscle tissue. This staining technique colors collagen fibers blue, while muscle fibers and red blood cells are colored red. This allows for the identification of collagen fibers and muscle fibers, as well as the visualization of collagen fiber content in different tissues. There was no obvious atherosclerosis and collagenization in myocardial tissue in the control group. It was severely atherosclerotic with obvious collagenization in the model group. In addition, this tissue in the Pro group was slightly atherosclerotic and collagenized. Moderate atherosclerosis and collagenization were observed in the myocardial tissue in the XDI-L group. Finally, the myocardial tissue in the XDI group was mildly atherosclerotic and collagenized ($p < 0.01$).

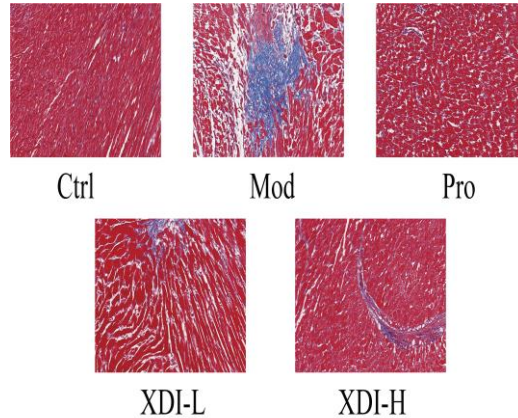


Figure 13: Masson staining

Table 2: Effects of XDI on fibrinogen deposition rate in rats with ISO-induced AMI ($\bar{X} \pm s$, $n=3$)

Group	Area of fibrosis/%
Ctrl	3.15 ± 1.27
Mod	$13.05 \pm 0.8^{##}$
Pro	$5.18 \pm 1.27^{**}$
XDI-L	$8.27 \pm 0.6^{**}$
XDI-H	$6.2 \pm 0.76^{**}$

Note: Compared with the Ctrl group, $^{##}P < 0.01$, Compared with the Mod group, $^{**}P < 0.01$.

4.11 Effect of XDI on serum levels of IL-6, LDH, ROS, IL-10, TNF- α , and cTn-I in AMI rats

The results showed that the serum levels of IL-6, LDH, ROS, TNF- α , and cTn-I significantly increased ($P<0.01$) but the serum level of IL-10 significantly decreased ($P<0.01$) in the model group, when compared to the ctrl group. Compared to the model group, the serum levels of IL-6, LDH, TNF- α , cTn-I ($P<0.01$), ROS ($P<0.05$), and IL-10 ($P<0.01$) decreased in the Pro group but increased in the XDI-L and XDI-H groups (Figure 14).

4.12 Effect of XDI on MDA and SOD levels in myocardial tissue of AMI rats

The results indicated that the SOD activity decreased ($P<0.01$) and the MAD activity increased ($P<0.01$), compared with the ctrl group. Moreover, the SOD activity increased and the MDA activity decreased in the Pro, XDI-M, and XDI-H groups, when compared to the model group ($P<0.01$) (see Figure 14).

Note: Compared with the Ctrl group, ## $P<0.01$, Compared with the Mod group, ** $P<0.01$.

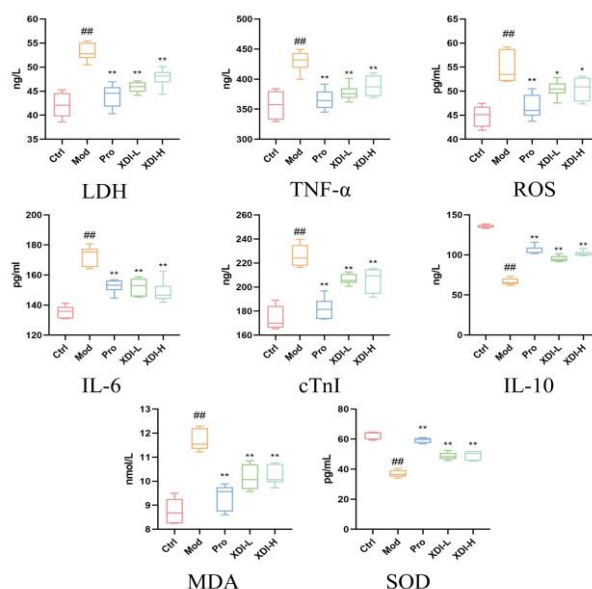


Figure 14: The serum levels of of IL-6,LDH,ROS,IL-10,TNF- α , and cTn-I (n=6)

5. Discussion

AMI is a pathological manifestation that causes abnormal energy metabolism of myocardial cells due to lack of oxygen and insufficient blood flow in the heart, resulting in the inability to maintain the normal function of the heart.

In this study, UPLC-Q-TOF-MS technology, network pharmacology, and molecular docking methods were used to predict and analyze the pharmacodynamic substances and mechanism of action of XDI in the treatment of AMI. The analysis of the "active ingredient-target-pathway" network showed that active blood-entering components such as Monomethyl lithospermate, Lithospermic acid, Esculentoside I, 6-O-galloylarbutin, Butylphthalide, and Tunicyclin A may play an important role in the efficacy of AMI treatment by in XDI. Monomethyl lithospermate is a compound extracted from *Salvia miltiorrhiza* with a variety of pharmacological activities such as antioxidant, anti-inflammatory,

and cardioprotective, and studies have shown that Monomethyl lithospermate significantly improves neurological damage caused by ischemia[5]. Lithospermic acid is a polycyclic phenol carboxylic acid isolated from *Salvia miltiorrhizae*; studies have shown that lithospermic acid can reduce cardiomyocyte damage by reducing oxidative stress and cardiomyocyte apoptosis[6]. Butylphthalide is a drug for the treatment of acute ischemic stroke; studies have shown that it can delay inflammation and antithrombosis and also exhibit anti-inflammatory and immunomodulatory effects[7,8]. *Bergenia stracheyi* contains 6-O-galloylarbutin, which has been shown to have antioxidant effects[9].

The results of KEGG enrichment analysis showed that the potential targets of XDI for the treatment of AMI mainly involved pathways, including lipid and atherosclerosis, the AGE-RAGE signaling pathway in diabetic complications, and the TNF signaling pathway. TNF works through two receptors, TNFR1 and TNFR2, the most classic of which is the activation of the NF- κ B and c-Jun pathways. Studies have shown that can effectively reduce myocardial injury in rats with myocardial infarction by downregulating the expression of TNF- α [10].

The analysis of the PPI network in this study revealed that TNF, ALB, EGFR, BCL2, SRC, STAT3, and other proteins were identified as the core targets of XDI in the treatment of AMI. The treatment primarily affects inflammatory response, myocardial fibrosis, angiogenesis, and other associated mechanisms. TNF is an inflammatory cytokine produced by macrophages or monocytes during acute inflammation[11]. Studies have shown that inhibiting the expression of TNF- α can effectively reduce inflammation and myocardial injury caused by myocardial ischemia[12]. Upon exposure to ischemic tissue, the amino terminus of ALB is altered to form ischemia-modified albumin (IMA), which is the only FDA-approved biomarker for the detection of tissue ischemia[13]. STAT3 is closely related to myocardial ischemia, and studies have shown that STAT3 gene knockout induces myocardial ischemia in mice[14,15]. Moreover, STAT3 activation can be observed in ischemia models.

The study results showed that XDI significantly reduced the serum levels of LDH, cTn-I, ROS, IL-10, IL-6, and TNF- α , reduced the level of MDA in myocardial tissue, and increased the level of SOD in myocardial tissue, compared to the model group. LDH is abundant in myocardial tissue, and the release of LDH is often caused by myocardial ischemia and hypoxia[16]. cTn-I is a biomarker that specifically indicates heart-related conditions and is considered the most reliable method for diagnosing acute coronary syndromes[17]. Oxidative stress refers to the mechanism by which ROS produces intracellular and extracellular toxic effects; studies have shown that AMI produces ROS, which causes oxidative stress and aggravates cardiomyocyte damage[18]. IL-10, IL-6, and TNF- α are pro-inflammatory factors associated with cardiovascular disease, and studies have shown that reducing the inflammatory response can effectively reduce myocardial damage[19]. SOD is one of the main components that directly scavenge oxygen free radicals in the body, and the activity of MDA indirectly reflects the severity of oxidative stress damage to body cells[20].

6. Conclusion

The experimental findings were validated through animal experiments, confirming the significant role of Monomethyl lithospermate, Lithospermic acid, Esculentoside I, 6-O-galloylarbutin, Butylphthalide, and Tunicyclin A in the treatment of AMI. Among them, EGFR-Monomethyl lithospermate, EGFR-Lithospermic acid, EGFR-6_O_galloylarbutin, and EGFR-Esculentoside I molecules were well combined, which can effectively protect isoproterenol-induced AMI rats.

References

- [1] Gibbons R J. Myocardial Ischemia in the Management of Chronic Coronary Artery Disease: Past and Present[J]. *Circ Cardiovasc Imaging*, 2021,14(1):e11615.
- [2] Jun L. Clinical Efficacy of Xiangdan Injection Combined with Atorvastatin Calcium Tablets in the Treatment of Coronary Heart Disease[J]. *Chinese Journal of Clinical Rational Drug Use*, 2024,17(14):11-14.
- [3] Xiang W X G Y. Research Progress on Main Components and Pharmacological Activities of *Dalbergia odorifera*[J]. *Special Wild Economic Animal and Plant Research*, 2023,45(06):143-150.
- [4] CONG M W S X. Advances in pharmacological research of *Salvia miltiorrhiza* and its drug pairs[J]. *Chinese Archives of Traditional Chinese Medicine*, 2024:1-8.
- [5] Yang F, Chen Z R, Yang X H, et al. Monomethyl lithospermate alleviates ischemic stroke injury in middle cerebral artery occlusion mice in vivo and protects oxygen glucose deprivation/reoxygenation induced SHSY-5Y cells in vitro via activation of PI3K/Akt signaling[J]. *Front Pharmacol*, 2022,13:1024439.
- [6] Zhang M, Wei L, Xie S, et al. Activation of Nrf2 by Lithospermic Acid Ameliorates Myocardial Ischemia and Reperfusion Injury by Promoting Phosphorylation of AMP-Activated Protein Kinase α (AMPK α)[J]. *Front Pharmacol*, 2021,12:794982.
- [7] Wang A, Jia B, Zhang X, et al. Efficacy and Safety of Butylphthalide in Patients With Acute Ischemic Stroke: A Randomized Clinical Trial[J]. *JAMA Neurol*, 2023,80(8):851-859.
- [8] Zhang Y, Ren Y, Chen X, et al. Role of Butylphthalide in Immunity and Inflammation: Butylphthalide May Be a Potential Therapy for Anti-Inflammation and Immunoregulation[J]. *Oxid Med Cell Longev*, 2022,2022:7232457.
- [9] Hou Y, Ali I, Li Z, et al. Separation of constituents from *Bergenia stracheyi* (Hook. F. & Thoms.) Engl. by high-speed countercurrent chromatography with elution mode and its antidiabetic and antioxidant in vitro evaluation[J]. *J Sep Sci*, 2021,44(3):767-776.
- [10] Cheng L Z W L. Mechanism of Zhishi Xiebai Guizhitang in Alleviating Myocardial Injury in Rats with Myocardial Infarction Based on TNF/NF- κ B Signaling Pathway[J]. *Chinese Journal of Experimental Traditional Medical Formulae*, 2023,29(18):8-16.
- [11] Idriss H T, Naismith J H. TNF α and the TNF receptor superfamily: structure-function relationship(s)[J]. *Microsc Res Tech*, 2000,50(3):184-195.
- [12] Yang W X, Chen L Y, Yang J L, et al. [Effect of different electrical current intensities of electroacupuncture preconditioning on cardiac function and macrophage polarization in mice with acute myocardial ischemia][J]. *Zhen Ci Yan Jiu*, 2022,47(11):955-961.
- [13] Bar-Or D, Lau E, Winkler J V. A novel assay for cobalt-albumin binding and its potential as a marker for myocardial ischemia-a preliminary report[J]. *J Emerg Med*, 2000,19(4):311-315.
- [14] Boengler K, Buechert A, Heinen Y, et al. Cardioprotection by ischemic postconditioning is lost in aged and STAT3-deficient mice[J]. *Circ Res*, 2008,102(1):131-135.
- [15] Xuan Y T, Guo Y, Han H, et al. An essential role of the JAK-STAT pathway in ischemic preconditioning[J]. *Proc Natl Acad Sci U S A*, 2001,98(16):9050-9055.
- [16] Fontes J P, Gonçalves M, Ribeiro V G. [Serum markers for ischemic myocardial damage][J]. *Rev Port Cardiol*, 1999,18(12):1129-1136.
- [17] Mingels A M, Gorgels T P, van Dieijen-Visser M P. [Cardiac troponin][J]. *Ned Tijdschr Geneesk*, 2012,156(42):A5044.
- [18] Misra M K, Sarwat M, Bhakuni P, et al. Oxidative stress and ischemic myocardial syndromes[J]. *Med Sci Monit*, 2009,15(10):A209-A219.
- [19] Zhang H, Dhalla N S. The Role of Pro-Inflammatory Cytokines in the Pathogenesis of Cardiovascular Disease[J]. *Int J Mol Sci*, 2024,25(2).
- [20] Yin Y, Han W, Cao Y. Association between activities of SOD, MDA and Na(+)-K(+)-ATPase in peripheral blood of patients with acute myocardial infarction and the complication of varying degrees of arrhythmia[J]. *Hellenic J Cardiol*, 2019,60(6):366-371.